ESRF	**Experiment title:** In-situ synchrotron study of the crystallization behavior of melt-spun WE54+Ni20 and the (de-)hydrogenation kinetics thereof	**Experiment number**: **MA1284**
Beamline: BM20	**Date of experiment**: from: 09.03.2011 to: 16.03.2011	**Date of report**: 11.07.11
Shifts: 18	**Local contact(s)**: Dr. Carsten Baehtz (baehtz@esrf.fr)	*Received at ESRF:*

Names and affiliations of applicants (* indicates experimentalists):

Lars Röntzsch*[1)], Siarhei Kalinichenka*[2)], Andreas Schmidt[1*)], Mathias Brauns[1*)].

1) Fraunhofer Institute for Manufacturing Technology and Applied Materials Research, Winterbergstraße 28, 01277 Dresden, Germany.

2) Institute for Materials Science, Dresden University of Technology, Helmholtzstraße 7, 01069 Dresden, Germany.

Report:

As it was shown recently the melt-spun WE54+Ni (75%Mg–5%Y–4%RE-16%Ni) alloy exhibits a remarkable blend of properties in view of its application as hydrogen solid-state storage material: At first a high reversible hydrogen storage capacity (nearly 6 wt.% -H_2) and secondly high (de-)hydrogenation rates of up to 1.3 wt.% -H_2 per minute. [1]. However, the phase transformation during crystallization and hydrogen (de)sorption of this new alloy have remained undetermined experimentally.

The aim of the in-situ diffraction study at the Rossendorf beamline ESRF-BM20 was to investiagte the crystal phase formation processes during thermal annealing of the amorphous as-spun WE54+Ni ($Mg_{90}Ni_8RE_2$, RE = Y, Nd, Gd), and furthermore, the desorption of hydrogeneted ribbons under vacuum, H_2 and Ar atmosphere. Thereby two kinds of samples were investigated: as-spun and hydrogenated $Mg_{90}Ni_8RE_2$ ribbon.

1. Crystal structure analysis of as-spun and (de)hydrogenated WE54+Ni ribbons.

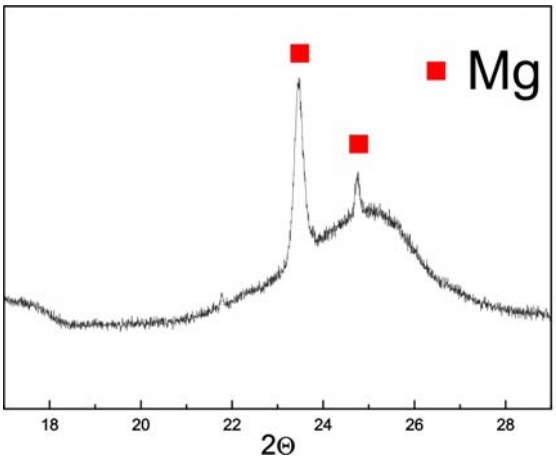

Fig. 1: SR-XRD spectra of as-spun WE54+Ni alloy.

Fig. 1 shows the SR-XRD pattern of the as-spun $Mg_{90}Ni_8RE_2$ ribbon. It can be seen a broad peak typical of an amorphous materials state and two weak reflections of crystalline hcp-Mg. A similar XRD pattern was observed in our previous studies of melt-spun Mg-Ni-Y and Mg-Cu-Y alloys [2, 3]. Consequently, the microstructure of the as-spun alloy is not fully amorphous. Fig. 3 shows the measured SR-XRD pattern of the hydrogenated (at 25 °C) and dehydrogenated (at 380 °C) $Mg_{90}Ni_8RE_2$ alloy. The hydrogenated alloy consists of four hydride phases (MgH_2, high temperature (HT) and low temperature (LT1) Mg_2NiH_4, $Mg_2NiH_{0.3}$ as well as crystalline Mg. The presence of Mg and $Mg_2NiH_{0.3}$ indicates the still incomplete hydrogenation of the sample at 300°C and 20 bar H_2 [1]. The XRD pattern for $Mg_{90}Ni_8RE_2$ after dehydrogenation reveals only the presence of hcp Mg and Mg_2Ni.

2. Time-resolved in-situ study of crystallization behavior of amorphous WE54+Ni ribbon.

The crystallization of the amorphous structure starts with growth of Mg grains at 100°C. The XRD data also shows that at 150°C the formation of metastable cubic Mg_6Ni phase occurs. Mg_6Ni decomposed at temperature of about 350 °C into Mg and Mg_2Ni [4, 5]. Furthermore, the presence of Ni_2Y_3 can be observed between 230 °C and 300 °C.
The final composition of the sample at 370 °C is Mg and Mg_2Ni. It is interesting that RE elements (such as Y, Nd or Gd), Zr or intermetallic phases containing them were not observed in the XRD pattern of the crystallized alloy, probably because of their small concentration or because they form a solid solution with Mg. The results of crystallization behavior of melt-spun Mg-Ni-Y provide very imortant information regarding the activation of as-spun ribbons [1].

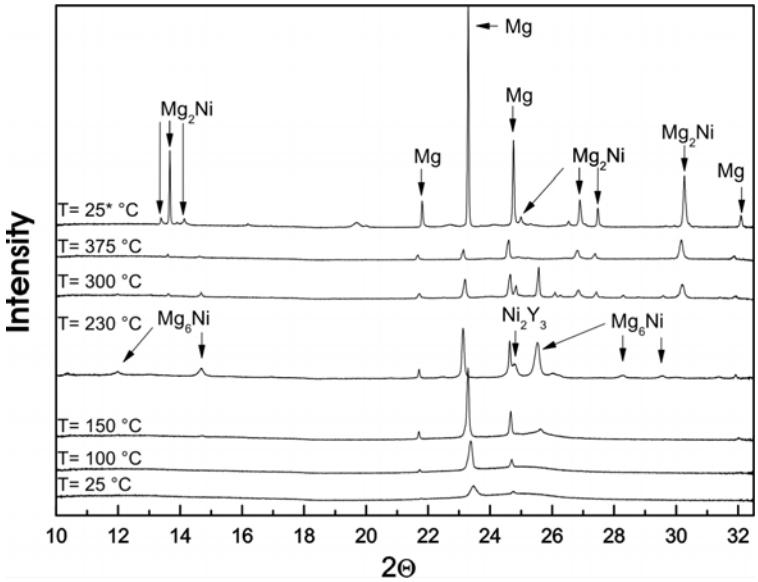

Fig. 2: Evolution of the in-situ SR-XRD pattern of the as spun WE54+Ni. The X-ray diffraction pattern at T = 25 °C* represents the X-ray diffraction pattern after crystallization.

3. Time-resolved in-situ XRD of hydrogen desorption of hydrogenated WE54+Ni ribbons.

The evolution of the SR-XRD pattern during hydrogen desorption of $Mg_{90}Ni_8RE_2$ is shown in Fig. 4. The incident X-ray beam with an X-ray wavelength of 1.05Å was used for investigation in the scanning range of the diffraction angle between 22.7 and 27.3° (2Θ) in reflection geometry. Additionally SR-XRD pattern of (de)hydrogenated $Mg_{90}Ni_8RE_2$ alloy are presented in Fig. 3.

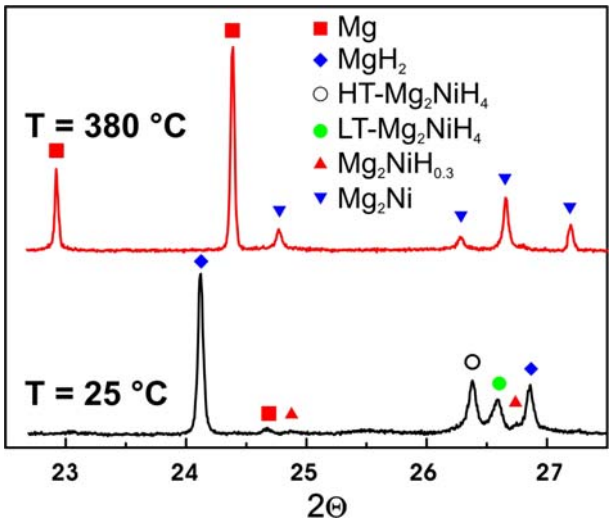

Fig. 3: SR-XRD pattern of hydrogenated $Mg_{90}Ni_8RE_2$ (25 °C) and of dehydrogenated $Mg_{90}Ni_8RE_2$ (385 °C).

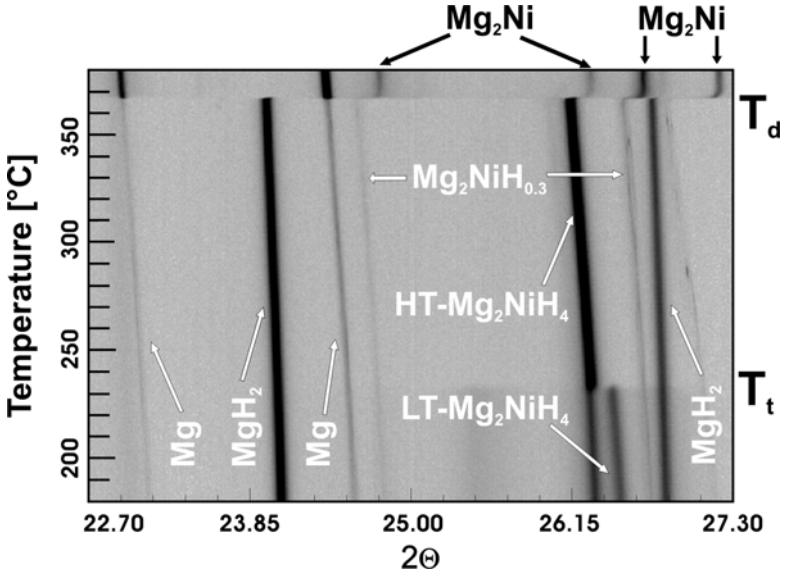

Fig. 4: Evolution of the in-situ SR-XRD pattern of the hydrogenated $Mg_{90}Ni_8RE_2$ up to 380 °C under vacuum (10^{-2} mbar).

According to the results obtained by SR-XRD $Mg_{90}Ni_8RE_2$ alloy undergoes a complex sequence of the phase transformations and the dehydrogenation reactions. On heating, the low temperature LT-Mg_2NiH_4 monoclinic phase changes into the high temperature HT-Mg_2NiH_4 cubic phase at 235 °C (T_t in Fig. 4). At 365 °C three separate processes were identified: desorption of Mg_2NiH_4, $Mg_2NiH_{0.3}$ and of MgH_2. These dehydrogenation reactions take place simultaneously. Thus, it is possible that $Mg_2NiH_{0.3}$ acts as a hydrogen transfer phase for the dehydrogenation of MgH_2, as it was found for Mg-Ni system [6].

Conclusion

Knowledge and understanding of the phase transformations and the dehydrogenation reactions of the melt-spun WE-Ni alloys may provide important insight into the mechanism behind the enhanced hydrogen storage properties of this system. The crystallization and desorption properties of $Mg_{90}Ni_8RE_2$ were studied by in-situ synchrotron X-ray diffraction performed at the Rossendorf Beamline (BM20) of the ESRF. The results obtained are summarized as follows:

1) As-spun $Mg_{90}Ni_8RE_2$ consists of Mg nanocrystals and an amorphous phase.
2) During crystallization of the amorphous structure the formation of Mg_2Ni, Mg_6Ni and Ni_2Y_3 was observed. Ni_2Y_3 and Mg_6Ni decomposed at temperature of about 350 °C.
3) In the case of $Mg_{90}Ni_8RE_2$ three separate processes were identified: desorption of Mg_2NiH_4 to $Mg_2NiH_{0.3}$ and desorption of MgH_2 in the presence of $Mg_2NiH_{0.3}$. Presumably, this should be attributed to the hydrogen transfer throug $Mg_2NiH_{0.3}$.

The results of these investigations will be published in the near future [7].

Acknowledgement

The authors would like to acknowledge financial support of the European Synchrotron Radiation Facility.

References

[1] S. Kalinichenka, L. Rontzsch, Th. Riedl, Th. Weißgärber, B. Kieback,, Hydrogen storage properties and microstructure of melt-spun $Mg_{90}Ni_8RE_2$ (RE = Y, Nd, Gd), Intl. J. Hydrogen Energy, Article in Press, DOI: 10.1016/j.ijhydene.2011.05.147..

[2] S. Kalinichenka, L. Röntzsch, B. Kieback, Structural and hydrogen storage properties of melt-spun Mg–Ni–Y alloys, Intl. J. Hydrogen Energy 34 (2009) 7749.

[3] S. Kalinichenka, L. Röntzsch, Th. Riedl, Th. Gemming, Th. Weißgärber, B. Kieback, Microstructure and hydrogen storage properties of melt-spun Mg-Cu-Ni-Y alloys, Intl. J. Hydrogen Energy 36 (2011)

[4] T. Spassov, St. Todorova, V. Petkov, Kinetics of Mg_6Ni nanocrystallization in amorphous $Mg_{83}Ni_{17}$, J. Non-Cryst. Sol. 355(2009) 1.

[5] A. Teresiak, M. Uhlemann, J. Thomas, A. Gebert, The metastable Mg_6Ni phase—Thermal behaviour, crystal structure and hydrogen reactivity of the rapidly quenched alloy, J. Alloys Comp, 475 (2009) 191.

[6] S. Kalinichenka, L. Rontzsch, C. Baehtz, B. Kieback, Hydrogen desorption kinetics of melt-spun and hydrogenated $Mg_{90}Ni_{10}$ and $Mg_{80}Ni_{10}Y_{10}$ using in situ synchrotron, X-ray diffraction and thermogravimetry, J. Alloys Comp, 496 (2010) 608.

[7] S. Kalinichenka, L. Röntzsch, B. Kieback, In situ TEM and XRD investigations of hydrogen desorption of melt-spun and hydrogenated $Mg_{90}Ni_8RE_2$ (RE = Y, Nd, Gd). In preparation.